DNA damage response protein TOPBP1 regulates X chromosome silencing in the mammalian germ line

Elias Ellnati[a], Helen R. Russell[b], Obah A. Ojarikre[a], Mahesh Sangrithi[c], Takayuki Hirota[a], Dirk G. de Rooij[d,e], Peter J. McKinnon[b], and James M. A. Turner[a,1]

[a]Sex Chromosome Biology Laboratory, The Francis Crick Institute, London NW1 1AT, United Kingdom; [b]Department of Genetics, St. Jude Children's Research Hospital, Memphis, TN 38105; [c]Department of Reproductive Medicine, KK Women's and Children's Hospital, 229899 Singapore; [d]Reproductive Biology Group, Division of Developmental Biology, Department of Biology, Faculty of Science, Utrecht University, 3584 CH Utrecht, The Netherlands; and [e]Center for Reproductive Medicine, Academic Medical Center, University of Amsterdam, Amsterdam 1105 AZ, The Netherlands

Edited by John J. Eppig, The Jackson Laboratory, Bar Harbor, ME, and approved October 18, 2017 (received for review July 14, 2017)

Meiotic synapsis and recombination between homologs permits the formation of cross-overs that are essential for generating chromosomally balanced sperm and eggs. In mammals, surveillance mechanisms eliminate meiotic cells with defective synapsis, thereby minimizing transmission of aneuploidy. One such surveillance mechanism is meiotic silencing, the inactivation of genes located on asynapsed chromosomes, via ATR-dependent serine-139 phosphorylation of histone H2AFX (γH2AFX). Stimulation of ATR activity requires direct interaction with an ATR activation domain (AAD)-containing partner. However, which partner facilitates the meiotic silencing properties of ATR is unknown. Focusing on the best-characterized example of meiotic silencing, meiotic sex chromosome inactivation, we reveal this AAD-containing partner to be the DNA damage and checkpoint protein TOPBP1. Conditional TOPBP1 deletion during pachynema causes germ cell elimination associated with defective X chromosome gene silencing and sex chromosome condensation. TOPBP1 is essential for localization to the X chromosome of silencing "sensors," including BRCA1, and effectors, including ATR, γH2AFX, and canonical repressive histone marks. We present evidence that persistent DNA double-strand breaks act as silencing initiation sites. Our study identifies TOPBP1 as a critical factor in meiotic sex chromosome silencing.

TOPBP1 | DNA damage | meiosis | meiotic silencing | spermatogenesis

Meiosis is the process by which haploid gametes are generated from diploid germ cells (1, 2). It comprises a single phase of DNA replication followed by two successive cell divisions. The first division is reductional, separating homologous chromosomes, whereas the second is equational, segregating sister chromatids. Before the first meiotic division, during prophase I, homologous chromosomes synapse and recombine. These processes together result in the formation of cross-overs, which permit accurate chromosome segregation and generate genetic diversity in offspring.

At early pachynema in male mammals, homologous autosomes are fully synapsed. In contrast, the X and Y chromosomes synapse only at a region of limited sequence homology, the pseudoautosomal region (PAR) (3) (Fig. S1*A*). The remaining, asynapsed chromosome regions undergo meiotic sex chromosome inactivation (MSCI), resulting in silencing of XY genes and formation of the sex body (4–7) (Fig. S1*A*). MSCI is essential for spermatogenesis (8), and aberrations in this process contribute to infertility in sex chromosome aneuploid models, interspecific hybrids, and targeted mutants defective in synapsis or recombination (9–12).

Although a hallmark of spermatocytes, silencing of asynapsed chromosomes is confined neither to the X and Y chromosomes nor to males. Any chromosome region asynapsed in males or females is inactivated (13, 14) by a process referred to as meiotic silencing (15). Meiotic silencing is suggested to restrict double-strand break (DSB) formation (7), prevent nonhomologous recombination (4, 6, 15), and enable DSB repair (16) at sites of asynapsis. It may also serve a checkpoint function to eliminate germ cells with asynapsed chromosomes, thereby preventing aneuploidy in progeny (10). Finally, in males, MSCI may shield the asynapsed XY chromosome regions from a synapsis checkpoint (17).

Meiotic silencing involves multiple DNA damage response (DDR) proteins, which function in two key steps. First, asynapsis is detected by "sensors," which localize to the axial elements (AEs). Subsequently, asynapsis signaling is transmitted to "effectors," which reside in the associated chromatin loops and cause long-range gene silencing. Based on their localization to the inactive XY bivalent, many potential sensors and effectors have been identified (4–6, 15, 18). Among these are the sensors SYCP3 (19), HORMAD1 (20), HORMAD2 (21), and BRCA1 (22), and the effectors MDC1 (23) and histone H2AFX (24). A critical link between sensors and effectors is provided by the DNA damage kinase ATR (25). SYCP3, HORMAD1, HORMAD2, and BRCA1 first recruit ATR to asynapsed AEs. Subsequently, ATR, facilitated by MDC1, translocates along chromatin loops, effecting gene silencing via phosphorylation of H2AFX at serine 139 (γH2AFX).

To fulfill its DNA repair and checkpoint functions, ATR must first be activated by proteins harboring an ATR activation domain (AAD). Two AAD-containing proteins, ETAA1 (26–29) and TOPBP1 (30, 31), act via independent pathways to activate ATR during mitosis (32–37). In contrast, the identity of the AAD-containing protein that activates ATR to initiate meiotic silencing is not known. ETAA1 expression during meiosis has not been examined. TOPBP1 is observed on the XY bivalent during pachynema (38, 39). However, the role of TOPBP1 in MSCI is

Significance

A fundamental step of meiosis is prophase I, when homologous chromosomes synapse and recombine to generate cross-overs that are accurate for chromosome segregation. In male mammals, chromosomes that are asynapsed undergo meiotic silencing, a process that may serve as a surveillance mechanism to prevent aneuploidy in offspring. We identify TOPBP1 as a factor involved in meiotic silencing. Deletion of TOPBP1 in male germ cells results in germ cell loss and failure to silence asynapsed chromosomes. We find that TOPBP1 acts at multiple stages in the silencing pathway. Our study highlights that TOPBP1 regulates sex chromosome expression in mammalian germ cells.

Author contributions: E.E. and J.M.A.T. designed research; E.E. and O.A.O. performed research; E.E., M.S., D.G.d.R., and J.M.A.T. analyzed data; H.R.R. and P.J.M. generated Topbp1 conditional mouse; and E.E., H.R.R., T.H., P.J.M., and J.M.A.T. wrote the paper.

The authors declare no conflict of interest.

This article is a PNAS Direct Submission.

[1]To whom correspondence should be addressed. Email: james.turner@crick.ac.uk.

This article contains supporting information online at www.pnas.org/lookup/suppl/doi:10.1073/pnas.1712530114/-/DCSupplemental.

unclear because mice carrying homozygous *Topbp1* deletions or AAD point mutations die during early embryogenesis (40–42).

By using a conditional deletion strategy, we now identify TOPBP1 as the ATR partner in meiotic silencing. We find that TOPBP1 directs assembly of multiple sensors and effectors at the XY pair. Thus, in addition to its roles in DNA damage repair and checkpoint signaling, TOPBP1 is an epigenetic regulator of sex chromosome expression in the mammalian germ line.

Results

To assess potential roles of *Topbp1* and *Etaa1* in MSCI, we studied their RNA expression and immunolocalization during spermatogenesis. We first examined RNA-sequencing (RNA-seq) datasets from isolated mouse spermatogonia, spermatocytes, and spermatids (43). The expression profile of *Topbp1* was similar to that of established MSCI effectors *Atr*, *Mdc1*, and *H2afx*, with transcript levels highest in spermatocytes (Fig. S1*B*). In contrast, *Etaa1* expression was relatively low in all germ cell subtypes and was decreased in spermatocytes relative to spermatogonia (Fig. S1*B*). By using combined antibody staining for TOPBP1 and SYCP3 on spermatocyte spreads, we confirmed previous reports that TOPBP1 localizes to the XY bivalent and is absent at the PAR (38, 39) (Fig. S1*C*; legend provides quantification). We also found that the dynamics of sex chromosome TOPBP1 localization matched that of ATR (Fig. S1*C*). TOPBP1 and ATR colocalized on the asynapsed regions of the XY pair during early, mid-, and late pachynema before disappearing at diplonema. In contrast, no localization of ETAA1 to the XY pair was observed (Fig. S1*D*). TOPBP1 was therefore a superior candidate to ETAA1 for regulating MSCI.

To determine whether TOPBP1 is required for XY silencing, we generated male mice carrying one *Topbp1* floxed and one *Topbp1* null allele (*Topbp1*$^{flox/-}$) (44), together with an *Ngn3 Cre* transgene that drives Cre recombinase expression in germ cells from postnatal day (P) 7 (breeding scheme presented in *Materials and Methods*) (45, 46). P42 testis weights in resulting *Topbp1*$^{flox/-}$ *Ngn3 Cre* males [hereafter *Topbp1* conditional KO (cKO)] were reduced fivefold relative to those in *Topbp1*$^{flox/+}$*Ngn3 Cre* males (hereafter control; Fig. 1*A*), whereas body weights were similar between these genotypes (Fig. S1*E*). TOPBP1 protein expression was markedly lower in *Topbp1* cKO than in control testes (Fig. 1*B*). *Topbp1* cKO seminiferous tubules exhibited a deficiency of spermatogonia and spermatocytes, and spermatids were rarely seen (Fig. 1*C*). Germ cell elimination in MSCI-deficient mutants occurs at midpachynema, or stage IV of the seminiferous cycle (47). As accurate tubule staging requires the presence of spermatogonia, which, in our model, were present in low numbers, we used an alternative approach to determine whether spermatocytes deficient in TOPBP1 were eliminated at midpachynema. TOPBP1 XY immunolocalization was compared between *Topbp1* cKO spermatocytes at early and late pachynema. At early pachynema, 60% of *Topbp1* cKO spermatocytes showed complete or partial loss of TOPBP1 from the XY bivalent, whereas the remaining 40% exhibited grossly unaffected TOPBP1 localization (Fig. 1*D*). However, at late pachynema, 100% of *Topbp1* cKO spermatocytes showed normal TOPBP1 XY localization (Fig. S1*F*). Spermatocytes exhibiting complete or partial loss of XY-associated TOPBP1 are therefore eliminated during midpachynema. As noted previously (8), we also observed in *Topbp1* cKO males loss of unaffected germ cells as a result of a bystander effect (*SI Results*).

We next used immunofluorescence to investigate relationships between TOPBP1 and meiotic silencing sensors SYCP3, HORMAD1, and HORMAD2 in early pachytene (EP) *Topbp1* cKO spermatocytes. We focused on cells with normal autosomal synapsis because asynapsed autosomes can indirectly disrupt MSCI by titrating silencing factors from the XY bivalent (9). Inclusion of an antibody to TOPBP1 allowed us to determine the localization of each sensor in cells with partial TOPBP1 loss (see Figs. 1–5), as well as in cells with complete TOPBP1 loss (see Figs. S1–S7).

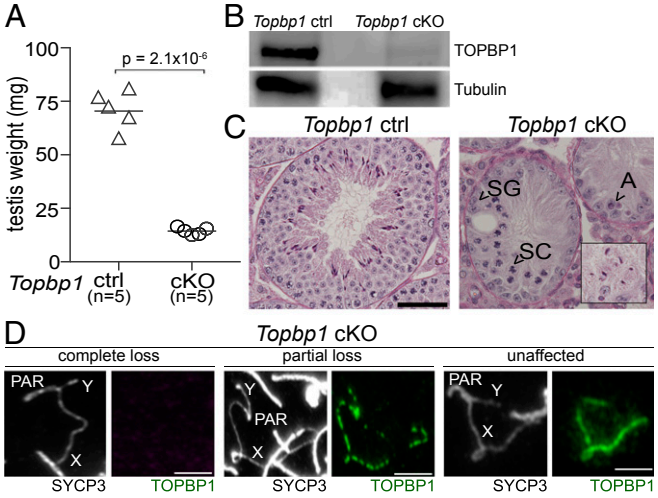

Fig. 1. TOPBP1 deletion causes germ cell loss. (*A*) Mean P42 testis weights ± SEM: 70.49 ± 4.60 mg for control and 14.40 ± 0.75 mg for *Topbp1* cKO. Each symbol represents the mean testis weight from one male. Significance was determined by unpaired *t* test. (*B*) Western blot for TOPBP1 in control and *Topbp1* cKO testes. Tubulin is used as loading control. (*C*) Periodic acid-Schiff–stained seminiferous tubule sections showing normal spermatogenesis in control and loss of spermatogonia and spermatocytes in *Topbp1* cKO males. A, apoptotic spermatocyte; SC, spermatocyte; SG, spermatogonia. (*Inset*) Presence of spermatids in some tubules from *Topbp1* cKO males. (*D*) *Topbp1* cKO XY bivalents at early pachynema showing complete TOPBP1 loss (*Left*), partial TOPBP1 loss (defined as regions of TOPBP1 discontinuity on the asynapsed XY axes; *Middle*), and unaffected TOPBP1 localization (*Right*; *n* = 3 males, *n* = 186 cells). (Scale bars, *C*, 50 μm; *D*, 5 μm.)

Accumulation of SYCP3 (Fig. S2*A*), HORMAD1 (Fig. S2*A*), and HORMAD2 (Fig. S2*B*) to XY AEs was unaffected by TOPBP1 depletion. These findings demonstrate that TOPBP1 lies downstream of SYCP3, HORMAD1, and HORMAD2 in the meiotic silencing pathway.

SYCP3 and HORMAD2 also label asynapsed autosomes. This localization pattern was unaffected in *Topbp1* cKO cells. We therefore used SYCP3/HORMAD2 immunostaining to determine whether TOPBP1 regulates synapsis. Addition of a TOPBP1 antibody again allowed us to compare phenotypes in cells with different extents of XY-associated TOPBP1 depletion. Normal synapsis occurred in 95% of *Topbp1* cKO cells with unaffected XY TOPBP1 localization, a frequency similar to that observed in controls (91%; Fig. S3). In contrast, normal synapsis was observed in only 46% and 52% of *Topbp1* cKO cells with partial and complete XY-associated TOPBP1 loss, respectively (Fig. S3). In the remaining cells, asynapsis affected the XY pair or the autosomes. TOPBP1 is therefore required for autosomal and XY synapsis.

Next, we examined XY localization of silencing factors ATR and BRCA1. Interestingly, ATR localization to the XY pair was compromised in *Topbp1* cKO cells. We observed a strict correspondence between TOPBP1 and ATR localization patterns: in cells with partial TOPBP1 depletion, regions of the XY AEs positive for TOPBP1 were positive for ATR, whereas regions lacking TOPBP1 lacked ATR (Fig. 2*A*). In cells with complete TOPBP1 loss, ATR was undetectable (Fig. S2*C*). Similarly, in TOPBP1-depleted cells, loading of BRCA1 to the XY bivalent was deficient except at regions where presumptive TOPBP1 was located (Fig. 2*B* and Fig. S2*D*; note that ATR acts as a TOPBP1 proxy in this experiment, as detailed in the legend to Fig. 2). XY localization of RBBP8, a partner of TOPBP1 (48) and BRCA1 (49, 50), was also defective in TOPBP1-depleted cells (Fig. 2*C* and Fig. S2*E*). Furthermore, serine-271 phosphorylation of HORMAD2 (pHORMAD2^{Ser271}), which is mediated by ATR (25), was compromised in *Topbp1* cKO cells (Fig. 2*D* and Fig. S2*F*),

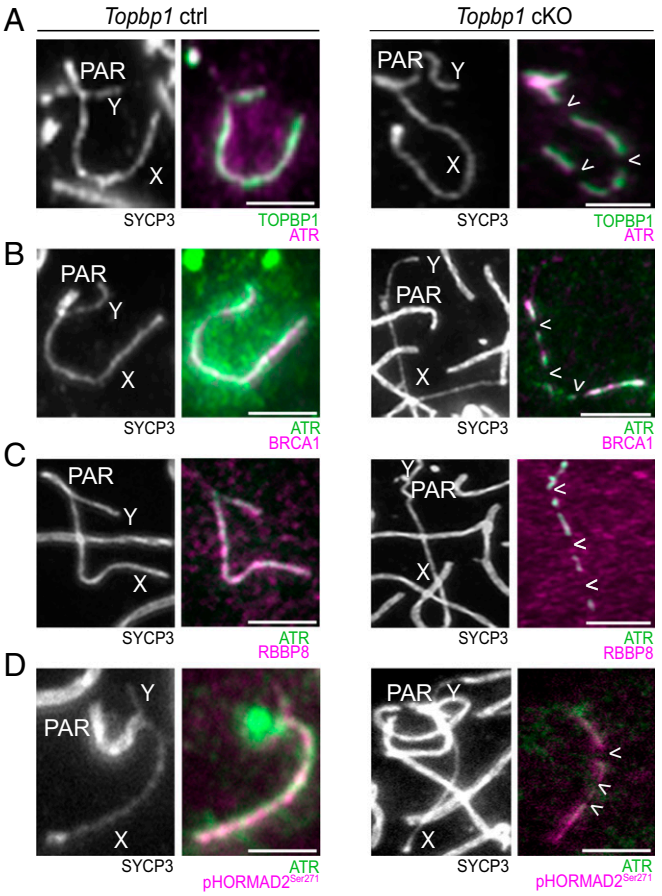

Fig. 2. TOPBP1 regulates localization of silencing sensors at XY AEs. (*A–D*) Immunostaining of meiotic chromosome spreads at early pachynema for SYCP3 (gray), TOPBP1 (green), and indicated silencing sensors (magenta) in control (*Left*; $n = 2$ males, $n = 50$ cells for each silencing sensor) and *Topbp1* cKO spermatocytes with partial TOPBP1 loss (*Right*; $n = 2$ males, $n = 55$, 52, 60, and 45 cells for ATR, BRCA1, RBBP8, and pHORMAD2^{Ser271}, respectively). Arrowheads indicate regions of XY AEs that are depleted for TOPBP1. Colocalization of green and magenta appears in white. (*B–D*) ATR is used as TOPBP1 proxy, as TOPBP1, BRCA1, RBBP8, and pHORMAD2^{Ser271} antibodies are raised in the same species and therefore cannot be used in combined immunofluorescence. (Scale bars, 5 μm.)

consistent with TOPBP1 acting as a cofactor of ATR in silencing. TOPBP1 is therefore essential for region-by-region assembly of ATR, BRCA1, RBBP8, and pHORMAD2^{Ser271} at asynapsed XY axes.

We subsequently assessed XY localization of silencing effectors MDC1 and γH2AFX. In control EP cells, both factors formed a cloud marking the XY chromatin loops (Fig. 3 *A* and *B*). However, in *Topbp1* cKO cells, formation of MDC1 and γH2AFX clouds was impaired. Chromatin loops arising from TOPBP1-positive AE stretches were positive for MDC1 and γH2AFX, whereas those arising from TOPBP1-deficient AE stretches were not (Fig. 3 *A* and *B*). XY bivalents without TOPBP1 were devoid of both effectors (Fig. S4). These findings show that TOPBP1 connects the sensor and effector arms of the silencing response. Furthermore, they demonstrate that spreading of silencing effectors into chromatin loops initiates from multiple independent sites along the length of asynapsed AEs.

Following acquisition of MDC1 and γH2AFX, XY chromatin undergoes further remodeling involving removal of histone H2A lysine-119 monoubiquitination (H2AK119ub) by USP7 (51, 52), acquisition of histone H3 lysine-9 trimethylation (H3K9me3) (53), and conjugation of unidentified targets with polyubiquitination (polyub) (54) and sumoylation (SUMO-1) (55, 56). We performed immunostaining for USP7, H3K9me3, polyub, and SUMO-1 to determine which, if any, of these pathways is TOPBP1-dependent. In *Topbp1* cKO cells, all four factors were undetectable, even at regions where TOPBP1 (or its proxy ATR) was preserved (Fig. 3 *C–F*). Absence of these components at TOPBP1-positive locations

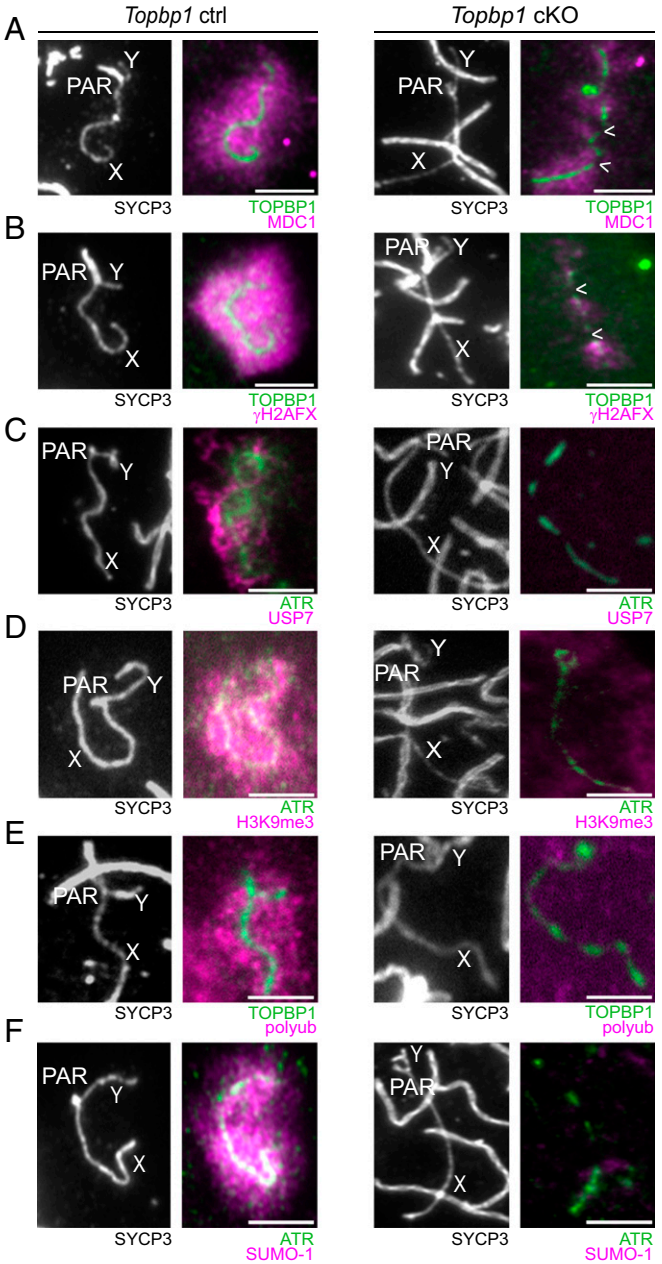

Fig. 3. TOPBP1 regulates localization of silencing effectors at XY chromatin loops. (*A–F*) Immunostaining of meiotic chromosome spreads at early pachynema using SYCP3 (gray), TOPBP1 (green), and indicated silencing effectors (magenta) in control (*Left*; $n = 2$ males, $n = 50$ cells for each silencing effector) and *Topbp1* cKO spermatocytes with partial TOPBP1 loss (*Right*; $n = 2$ males, $n = 51$, 53, 50, 47, 50, and 59 cells for MDC1, γH2AFX, USP7, H3K9me3, polyub, and SUMO-1, respectively). Arrowheads indicate regions of XY AEs that are depleted for TOPBP1. Colocalization of green and magenta appears in white. In *C*, *D*, and *F*, ATR is used as TOPBP1 proxy because TOPBP1, USP7, H3K9me3, and SUMO-1 antibodies are raised in the same species and therefore cannot be used in combined immunofluorescence. (Scale bars, 5 μm.)

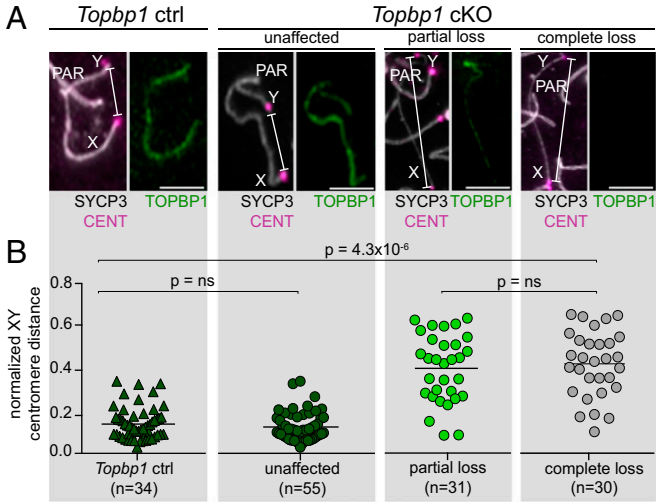

Fig. 4. Sex chromosome condensation is defective in *Topbp1* cKO spermatocytes. (*A*) Conformation of XY chromosome axes at early pachynema assessed in control spermatocytes and in *Topbp1* cKO spermatocytes with unaffected TOPBP1 localization, partial TOPBP1 loss, and complete TOPBP1 loss: SYCP3 (gray), TOPBP1 (green), centromeres (magenta). (*B*) Plots of linear distances between X and Y centromeres. The distance is normalized to the nuclear diameter. *P* values were calculated by one-way ANOVA. (Scale bars, 5 μm.)

may be the result of antibody inefficiencies, or because high levels of TOPBP1 are required for successful recruitment of these components. Either way, TOPBP1 lies upstream of USP7, H3K9me3, polyub, and SUMO-1 in the XY chromatin-remodeling pathways.

At early pachynema, the asynapsed X chromosome contains multiple persistent meiotic DSBs. These DSBs may act as initiation sites for silencing factor spreading (15, 57). Before investigating the potential relationship between DSBs and silencing, we first assessed whether global DSB abundance was perturbed in *Topbp1* cKO males. Leptotene focus counts for the DSB markers RPA subunit 2 (RPA2; Fig. S5*A*) and RAD51 (Fig. S5*B*) were similar to those in controls, indicating that DSB numbers in *Topbp1* cKO males were grossly unaffected. Focusing on EP *Topbp1* cKO cells with partial TOPBP1 loss, we then examined spatial proximity between the TOPBP1 proxy ATR and RPA2 foci along the X chromosome AE (Fig. S6). We noticed a striking colocalization between these DDR factors: 98% of AE stretches that were positive for ATR contained RPA2 foci, whereas only 3% of AE stretches that were negative for ATR contained RPA2 foci. Conversely, 99% of all X chromosome RPA2 foci resided within AE stretches that were positive for ATR. These findings support the hypothesis that DNA damage is the initiating lesion for meiotic silencing.

During MSCI, the X and Y chromosomes condense to form the sex body, in which their centromeres come into close proximity. Given the defects in localization of silencing factors to the XY pair in *Topbp1* cKO males, we suspected that sex body formation in these mice would be perturbed. To test this possibility, we used an established method (23) to compare the mean X-to-Y centromere distance between EP *Topbp1* cKO cells with differing extents of TOPBP1 depletion (Fig. 4). *Topbp1* cKO cells with unaffected TOPBP1 localization exhibited a mean X-to-Y centromere distance indistinguishable from that in controls, suggesting that they had achieved sex chromosome condensation. However, *Topbp1* cKO cells with complete TOPBP1 loss had a mean X-to-Y centromere distance threefold higher than controls. Interestingly, the mean X-to-Y centromere distance in *Topbp1* cKO cells with partial TOPBP1 loss was similar to that in cells with complete TOPBP1 loss. TOPBP1 colocalization to the XY bivalent must therefore exceed a threshold to initiate sex chromosome condensation.

Finally, we used RNA FISH to examine whether TOPBP1 is required for silencing of X genes at pachynema. We examined in *Topbp1* cKO and controls expression of genes located near the centromere (*Utx*), the center (*Zfx*), and the PAR (*Scml2*) of the X chromosome (Fig. 5*A*). Following RNA FISH, we performed immunostaining for HORMAD2 and γH2AFX. XY HORMAD2 localization, which is unaffected by TOPBP1 depletion (Fig. S2*B*), was used to identify pachytene cells by a method described previously (58, 59). Among the *Topbp1* cKO pachytene population, cells with TOPBP1 depletion were identified by virtue of having defective XY γH2AFX acquisition. We observed silencing of *Utx*, *Zfx*, and *Scml2* in almost all pachytene cells from control males (Fig. 5). However, expression of all three X genes persisted in TOPBP1-depleted pachytene cells (Fig. 5). Notably, the proportion of TOPBP1-deficient pachytene cells misexpressing *Utx*, *Zfx*, and *Scml2* was equivalent to that observed in an established MSCI mutant, the *H2afx*-null male (60) (Fig. 5). We conclude that meiotic X chromosome silencing requires TOPBP1.

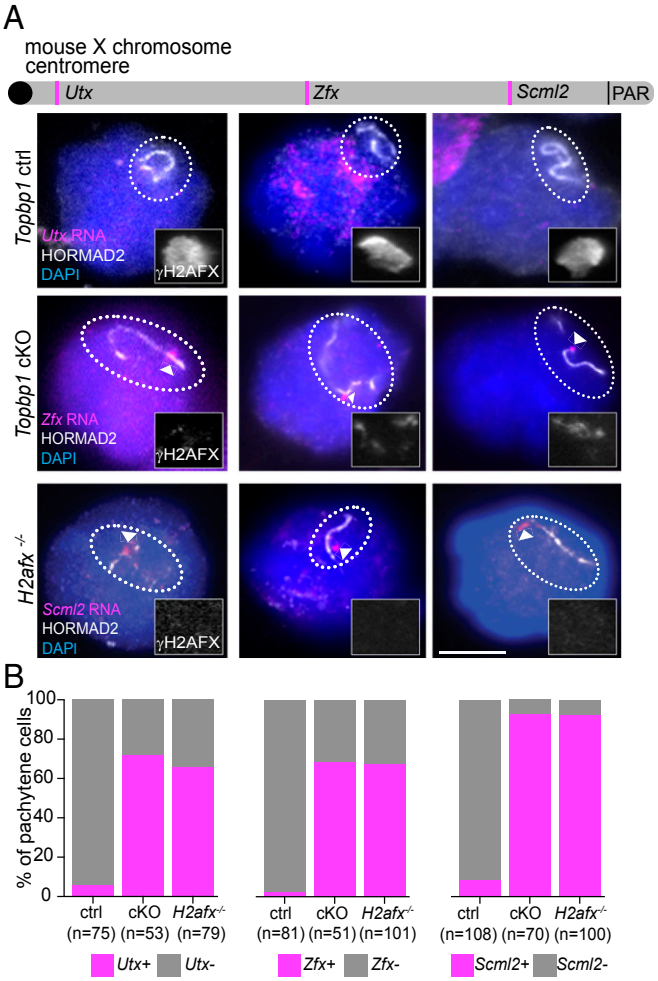

Fig. 5. TOPBP1 is required for MSCI. (*A*, *Top*) Mouse X chromosome showing the location of *Utx*, *Zfx*, and *Scml2*. RNA FISH images for each gene in control, *Topbp1* cKO, and *H2afx*$^{-/-}$ EP spermatocytes. Dotted circles enclose the X chromosome, for which γH2AFX immunostaining is shown (*Insets*). Arrowheads indicate *Utx*, *Zfx*, and *Scml2* RNA FISH signals ($n = 2$ males). (*B*) Graphs showing the proportion of EP spermatocytes expressing each gene in each genotype, with corresponding numbers of cells indicated. (Scale bars, 5 μm.)

Discussion

Aside from its well-established roles in DNA replication, DNA repair, and checkpoint control, TOPBP1 can interact with chromatin-remodeling complexes and transcription factors to influence gene expression (61). Here we show that TOPBP1 is also critical for meiotic silencing (Fig. S7), thereby supporting a role for this protein in epigenetic regulation. Although, in other contexts, TOPBP1 has functions that are independent of ATR (61), the meiotic silencing defects in TOPBP1-deficient males resemble those in ATR-deficient males (25). In both models, localization of early sensor components SYCP3, HORMAD1, and HORMAD2 to the XY pair is unaffected, whereas subsequent acquisition of BRCA1 and of the ATR-phosphortarget pHORMAD2Ser^{271} is perturbed. Furthermore, the same downstream effector pathways that enforce X-gene silencing are disrupted. Based on these phenotypic similarities, we suggest that TOPBP1 imparts its silencing functions principally as an ATR cofactor.

Notably, partial TOPBP1 depletion was sufficient to abolish sex chromosome condensation and silencing of X-linked genes. This finding suggests that MSCI is sensitive to the levels of silencing components. In support of this hypothesis, MSCI is perturbed by an increasing dose of asynapsed autosomes, which titrate silencing factors from the XY bivalent (9, 62). TOPBP1, like other silencing effectors ATR (63) and H2AFX (64), exhibits higher expression in testis than in somatic tissues (65). We suggest that elevated levels of silencing effectors TOPBP1, ATR, and H2AFX within spermatocytes reflect the unique requirement of these cells to inactivate hundreds of X and Y chromosome genes.

The existence in our *Topbp1* cKO mutant of pachytene cells with partial TOPBP1 depletion was fortuitous, as it allowed us to observe silencing initiation sites along the X chromosome AE. Two resulting observations were noteworthy. First, spreading of silencing factors initiates from multiple sites along the X chromosome axis. This mechanism contrasts with that observed during female somatic X chromosome inactivation, in which silencing components spread from a single site termed the X inactivation center (66). Second, on the meiotic X chromosome, silencing initiation sites coincide with DSB sites. Despite involving multiple DDR factors, meiotic silencing was originally thought to be DSB-independent because it also occurs in spermatocytes lacking the meiotic DSB-inducing enzyme SPO11 (64, 67, 68). However, DNA damage foci, the origin of which is unknown, have since been observed in *Spo11*-null pachytene spermatocytes, where they colocalize with silencing domains (57). Our findings build on these observations and provide compelling evidence that DSBs are meiotic silencing initiation sites.

We also show that TOPBP1 is essential for completion of autosomal and XY synapsis. The asynapsis phenotype in *Topbp1* cKO males could result from defective recombination, synaptonemal complex (SC) formation, or both. Although DSB abundance is unaffected in *Topbp1* cKO males at leptonema, we were unable to establish the extent of TOPBP1 depletion in individual spermatocytes at this stage. Further investigation of the role of TOPBP1 in recombination will therefore require a superior *Cre* driver. We find that TOPBP1 is required for serine-271 phosphorylation of the SC component HORMAD2. TOPBP1 may facilitate phosphorylation of other known ATR SC targets, as well as SC components with (S/T)Q cluster domains (69). Finally, we note that localization of ATR to the XY pair during meiosis is TOPBP1-dependent. This observation is intriguing, because assembly of ATR at sites of DNA damage during mitosis is TOPBP1-independent (70). The extent to which interrelationships between TOPBP1 and ATR differ in meiosis and mitosis is therefore an interesting avenue for future study.

Materials and Methods

Mice. All mice were maintained according to UK Home Office Regulations at the National Institute for Medical Research and the Francis Crick Institute Mill Hill laboratory. To generate *Topbp1*$^{flox/-}$ *Ngn3 Cre* males, we first mated conditional *Topbp1*$^{flox/+}$ females (44) to males carrying the *Ngn3 Cre* transgene (45, 46). In the germ line of resulting *Topbp1*$^{flox/+}$ *Ngn3 Cre* sons, Cre recombinase converts *Topbp1*^{flox} alleles into *Topbp1*$^{-}$ (i.e., null) alleles. Mating these males to *Topbp1*$^{flox/flox}$ females generates *Topbp1*$^{flox/-}$ *Ngn3 Cre* sons and *Topbp1*$^{flox/+}$ *Ngn3 Cre* control brothers. *Topbp1*^{flox} and *Ngn3 Cre* were maintained on a C57BL/6 background. *H2afx*$^{-/-}$ males (60) were maintained on an MF1 background.

RNA FISH, Immunofluorescence, and Western Blotting. RNA FISH digoxigenin-labeled probes were prepared from BAC DNA (from CHORI, *Scml2*, RP24-204O18; *Zfx*, RP24-204018; *Utx*, gift from Mike Mitchell, University Aix-Marseille, Marseille, France) as described previously (71). Immunofluorescence experiments were carried out as described previously (13) (*SI Materials and Methods* lists antibodies). Western blotting was carried out as described previously (72) with TOPBP1 and tubulin (T9026; Sigma) antibodies used at 1:1,000 and 1:14,000, respectively.

Microscopy. Imaging was performed by using an Olympus IX70 inverted microscope with a 100-W mercury arc lamp. An Olympus UPlanApo 100×/1.35 N.A. oil-immersion objective was used for meiotic chromosome spread and RNA FISH imaging. An Olympus UPlanApo 40×/0.75 N.A. objective was used for imaging testis sections. A DeltaVision RT computer-assisted Photometrics CoolSnap HQ CCD camera with an ICX285 Progressive scan CCD image sensor was used for capturing images. Fiji software was used to process 8- or 16-bit (512 × 512 or 1,024 × 1,024 pixels) captured images.

ACKNOWLEDGMENTS. We thank the Francis Crick Institute Biological Research, Light Microscopy, and Experimental Histopathology facilities for their expertise; Attila Tóth for the HORMAD1 and HORMAD2 antibodies; Bill Earnshaw for the CREST antibody; Satoshi Namekawa for the BRCA1 antibody; Mike Mitchell for the *Utx* BAC; Jasmin Zohren for statistical advice; and members of the laboratory of J.M.A.T. for comments on the manuscript. This study was supported by European Research Council Grant CoG 647971 (to J.M.A.T.); the Francis Crick Institute (J.M.A.T.), which receives its core funding (Grant FC001193) from Cancer Research UK, the UK Medical Research Council, and the Wellcome Trust; National Institutes of Health Grants NS-37956 (to P.J.M.) and CA-21765 (to P.J.M.); Cancer Center Support Grant Grant P30 CA21765 (to P.J.M.); and the American Lebanese and Syrian Associated Charities of St. Jude Children's Research Hospital.

1. Baudat F, Imai Y, de Massy B (2013) Meiotic recombination in mammals: Localization and regulation. *Nat Rev Genet* 14:794–806.
2. Handel MA, Schimenti JC (2010) Genetics of mammalian meiosis: Regulation, dynamics and impact on fertility. *Nat Rev Genet* 11:124–136.
3. Kauppi L, Jasin M, Keeney S (2012) The tricky path to recombining X and Y chromosomes in meiosis. *Ann N Y Acad Sci* 1267:18–23.
4. Ichijima Y, Sin HS, Namekawa SH (2012) Sex chromosome inactivation in germ cells: Emerging roles of DNA damage response pathways. *Cell Mol Life Sci* 69:2559–2572.
5. Yan W, McCarrey JR (2009) Sex chromosome inactivation in the male. *Epigenetics* 4: 452–456.
6. Inagaki A, Schoenmakers S, Baarends WM (2010) DNA double strand break repair, chromosome synapsis and transcriptional silencing in meiosis. *Epigenetics* 5:255–266.
7. McKee BD, Handel MA (1993) Sex chromosomes, recombination, and chromatin conformation. *Chromosoma* 102:71–80.
8. Royo H, et al. (2010) Evidence that meiotic sex chromosome inactivation is essential for male fertility. *Curr Biol* 20:2117–2123.
9. Mahadevaiah SK, et al. (2008) Extensive meiotic asynapsis in mice antagonises meiotic silencing of unsynapsed chromatin and consequently disrupts meiotic sex chromosome inactivation. *J Cell Biol* 182:263–276.
10. Burgoyne PS, Mahadevaiah SK, Turner JM (2009) The consequences of asynapsis for mammalian meiosis. *Nat Rev Genet* 10:207–216.
11. Bhattacharyya T, et al. (2013) Mechanistic basis of infertility of mouse intersubspecific hybrids. *Proc Natl Acad Sci USA* 110:E468–E477.
12. Campbell P, Good JM, Nachman MW (2013) Meiotic sex chromosome inactivation is disrupted in sterile hybrid male house mice. *Genetics* 193:819–828.
13. Turner JM, et al. (2005) Silencing of unsynapsed meiotic chromosomes in the mouse. *Nat Genet* 37:41–47.
14. Baarends WM, et al. (2005) Silencing of unpaired chromatin and histone H2A ubiquitination in mammalian meiosis. *Mol Cell Biol* 25:1041–1053.
15. Turner JM (2015) Meiotic silencing in mammals. *Annu Rev Genet* 49:395–412.
16. Lu LY, Yu X (2015) Double-strand break repair on sex chromosomes: Challenges during male meiotic prophase. *Cell Cycle* 14:516–525.
17. Jablonka E, Lamb MJ (1988) Meiotic pairing constraints and the activity of sex chromosomes. *J Theor Biol* 133:23–36.
18. Alavattam KG, et al. (2016) Elucidation of the Fanconi anemia protein network in meiosis and its function in the regulation of histone modifications. *Cell Rep* 17: 1141–1157.

19. Kouznetsova A, et al. (2009) BRCA1-mediated chromatin silencing is limited to oocytes with a small number of asynapsed chromosomes. *J Cell Sci* 122:2446–2452.
20. Daniel K, et al. (2011) Meiotic homologue alignment and its quality surveillance are controlled by mouse HORMAD1. *Nat Cell Biol* 13:599–610.
21. Wojtasz L, et al. (2012) Meiotic DNA double-strand breaks and chromosome asynapsis in mice are monitored by distinct HORMAD2-independent and -dependent mechanisms. *Genes Dev* 26:958–973.
22. Turner JM, et al. (2004) BRCA1, histone H2AX phosphorylation, and male meiotic sex chromosome inactivation. *Curr Biol* 14:2135–2142.
23. Ichijima Y, et al. (2011) MDC1 directs chromosome-wide silencing of the sex chromosomes in male germ cells. *Genes Dev* 25:959–971.
24. Fernandez-Capetillo O, et al. (2003) H2AX is required for chromatin remodeling and inactivation of sex chromosomes in male mouse meiosis. *Dev Cell* 4:497–508.
25. Royo H, et al. (2013) ATR acts stage specifically to regulate multiple aspects of mammalian meiotic silencing. *Genes Dev* 27:1484–1494.
26. Haahr P, et al. (2016) Activation of the ATR kinase by the RPA-binding protein ETAA1. *Nat Cell Biol* 18:1196–1207.
27. Bass TE, et al. (2016) ETAA1 acts at stalled replication forks to maintain genome integrity. *Nat Cell Biol* 18:1185–1195.
28. Feng S, et al. (2016) Ewing tumor-associated antigen 1 interacts with replication protein A to promote restart of stalled replication forks. *J Biol Chem* 291: 21956–21962.
29. Lee YC, Zhou Q, Chen J, Yuan J (2016) RPA-binding protein ETAA1 is an ATR activator involved in DNA replication stress response. *Curr Biol* 26:3257–3268.
30. Kumagai A, Lee J, Yoo HY, Dunphy WG (2006) TopBP1 activates the ATR-ATRIP complex. *Cell* 124:943–955.
31. Burrows AE, Elledge SJ (2008) How ATR turns on: TopBP1 goes on ATRIP with ATR. *Genes Dev* 22:1416–1421.
32. Delacroix S, Wagner JM, Kobayashi M, Yamamoto K, Karnitz LM (2007) The Rad9-Hus1-Rad1 (9-1-1) clamp activates checkpoint signaling via TopBP1. *Genes Dev* 21: 1472–1477.
33. Lee J, Kumagai A, Dunphy WG (2007) The Rad9-Hus1-Rad1 checkpoint clamp regulates interaction of TopBP1 with ATR. *J Biol Chem* 282:28036–28044.
34. Cotta-Ramusino C, et al. (2011) A DNA damage response screen identifies RHINO, a 9-1-1 and TopBP1 interacting protein required for ATR signaling. *Science* 332: 1313–1317.
35. Duursma AM, Driscoll R, Elias JE, Cimprich KA (2013) A role for the MRN complex in ATR activation via TOPBP1 recruitment. *Mol Cell* 50:116–122.
36. Zou L, Cortez D, Elledge SJ (2002) Regulation of ATR substrate selection by Rad17-dependent loading of Rad9 complexes onto chromatin. *Genes Dev* 16:198–208.
37. Zou L, Elledge SJ (2003) Sensing DNA damage through ATRIP recognition of RPA-ssDNA complexes. *Science* 300:1542–1548.
38. Perera D, et al. (2004) TopBP1 and ATR colocalization at meiotic chromosomes: Role of TopBP1/Cut5 in the meiotic recombination checkpoint. *Mol Biol Cell* 15:1568–1579.
39. Reini K, et al. (2004) TopBP1 localises to centrosomes in mitosis and to chromosome cores in meiosis. *Chromosoma* 112:323–330.
40. Jeon Y, et al. (2011) TopBP1 deficiency causes an early embryonic lethality and induces cellular senescence in primary cells. *J Biol Chem* 286:5414–5422.
41. Yamane K, Wu X, Chen J (2002) A DNA damage-regulated BRCT-containing protein, TopBP1, is required for cell survival. *Mol Cell Biol* 22:555–566.
42. Zhou ZW, et al. (2013) An essential function for the ATR-activation-domain (AAD) of TopBP1 in mouse development and cellular senescence. *PLoS Genet* 9:e1003702.
43. Gan H, et al. (2013) Integrative proteomic and transcriptomic analyses reveal multiple post-transcriptional regulatory mechanisms of mouse spermatogenesis. *Mol Cell Proteomics* 12:1144–1157.
44. Lee Y, et al. (2012) Neurogenesis requires TopBP1 to prevent catastrophic replicative DNA damage in early progenitors. *Nat Neurosci* 15:819–826.
45. Zheng K, Wang PJ (2012) Blockade of pachytene piRNA biogenesis reveals a novel requirement for maintaining post-meiotic germline genome integrity. *PLoS Genet* 8: e1003038.
46. Schonhoff SE, Giel-Moloney M, Leiter AB (2004) Neurogenin 3-expressing progenitor cells in the gastrointestinal tract differentiate into both endocrine and non-endocrine cell types. *Dev Biol* 270:443–454.
47. de Rooij DG, de Boer P (2003) Specific arrests of spermatogenesis in genetically modified and mutant mice. *Cytogenet Genome Res* 103:267–276.
48. Ramírez-Lugo JS, Yoo HY, Yoon SJ, Dunphy WG (2011) CtIP interacts with TopBP1 and Nbs1 in the response to double-stranded DNA breaks (DSBs) in Xenopus egg extracts. *Cell Cycle* 10:469–480.
49. Yu X, Wu LC, Bowcock AM, Aronheim A, Baer R (1998) The C-terminal (BRCT) domains of BRCA1 interact in vivo with CtIP, a protein implicated in the CtBP pathway of transcriptional repression. *J Biol Chem* 273:25388–25392.
50. Wong AK, et al. (1998) Characterization of a carboxy-terminal BRCA1 interacting protein. *Oncogene* 17:2279–2285.
51. Luo M, et al. (2015) Polycomb protein SCML2 associates with USP7 and counteracts histone H2A ubiquitination in the XY chromatin during male meiosis. *PLoS Genet* 11: e1004954.
52. Hasegawa K, et al. (2015) SCML2 establishes the male germline epigenome through regulation of histone H2A ubiquitination. *Dev Cell* 32:574–588.
53. Kato Y, et al. (2015) FANCB is essential in the male germline and regulates H3K9 methylation on the sex chromosomes during meiosis. *Hum Mol Genet* 24: 5234–5249.
54. Sin HS, et al. (2012) RNF8 regulates active epigenetic modifications and escape gene activation from inactive sex chromosomes in post-meiotic spermatids. *Genes Dev* 26: 2737–2748.
55. Vigodner M, Morris PL (2005) Testicular expression of small ubiquitin-related modifier-1 (SUMO-1) supports multiple roles in spermatogenesis: Silencing of sex chromosomes in spermatocytes, spermatid microtubule nucleation, and nuclear reshaping. *Dev Biol* 282:480–492.
56. Rogers RS, Inselman A, Handel MA, Matunis MJ (2004) SUMO modified proteins localize to the XY body of pachytene spermatocytes. *Chromosoma* 113:233–243.
57. Carofiglio F, et al. (2013) SPO11-independent DNA repair foci and their role in meiotic silencing. *PLoS Genet* 9:e1003538.
58. Cloutier JM, Mahadevaiah SK, Ellnati E, Toth A, Turner J (2015) Mammalian meiotic silencing exhibits sexually dimorphic features. *Chromosoma* 125:215–226.
59. Cloutier JM, et al. (2015) Histone H2AFX links meiotic chromosome asynapsis to prophase I oocyte loss in mammals. *PLoS Genet* 11:e1005462.
60. Celeste A, et al. (2002) Genomic instability in mice lacking histone H2AX. *Science* 296: 922–927.
61. Wardlaw CP, Carr AM, Oliver AW (2014) TopBP1: A BRCT-scaffold protein functioning in multiple cellular pathways. *DNA Repair (Amst)* 22:165–174.
62. Homolka D, Ivanek R, Capkova J, Jansa P, Forejt J (2007) Chromosomal rearrangement interferes with meiotic X chromosome inactivation. *Genome Res* 17:1431–1437.
63. Keegan KS, et al. (1996) The Atr and Atm protein kinases associate with different sites along meiotically pairing chromosomes. *Genes Dev* 10:2423–2437.
64. Mahadevaiah SK, et al. (2001) Recombinational DNA double-strand breaks in mice precede synapsis. *Nat Genet* 27:271–276.
65. Fagerberg L, et al. (2014) Analysis of the human tissue-specific expression by genome-wide integration of transcriptomics and antibody-based proteomics. *Mol Cell Proteomics* 13:397–406.
66. Gendrel AV, Heard E (2014) Noncoding RNAs and epigenetic mechanisms during X-chromosome inactivation. *Annu Rev Cell Dev Biol* 30:561–580.
67. Barchi M, et al. (2005) Surveillance of different recombination defects in mouse spermatocytes yields distinct responses despite elimination at an identical developmental stage. *Mol Cell Biol* 25:7203–7215.
68. Bellani MA, Romanienko PJ, Cairatti DA, Camerini-Otero RD (2005) SPO11 is required for sex-body formation, and Spo11 heterozygosity rescues the prophase arrest of Atm-/- spermatocytes. *J Cell Sci* 118:3233–3245.
69. Carballo JA, Cha RS (2007) Meiotic roles of Mec1, a budding yeast homolog of mammalian ATR/ATM. *Chromosome Res* 15:539–550.
70. Liu S, et al. (2006) Claspin operates downstream of TopBP1 to direct ATR signaling towards Chk1 activation. *Mol Cell Biol* 26:6056–6064.
71. Mahadevaiah SK, Costa Y, Turner JM (2009) Using RNA FISH to study gene expression during mammalian meiosis. *Methods Mol Biol* 558:433–444.
72. Hamer G, Kal HB, Westphal CH, Ashley T, de Rooij DG (2004) Ataxia telangiectasia mutated expression and activation in the testis. *Biol Reprod* 70:1206–1212.
73. Kim D, et al. (2013) TopHat2: Accurate alignment of transcriptomes in the presence of insertions, deletions and gene fusions. *Genome Biol* 14:R36.
74. Trapnell C, et al. (2013) Differential analysis of gene regulation at transcript resolution with RNA-seq. *Nat Biotechnol* 31:46–53.
75. Trapnell C, et al. (2012) Differential gene and transcript expression analysis of RNA-seq experiments with TopHat and Cufflinks. *Nat Protoc* 7:562–578.
76. Broering TJ, et al. (2014) BRCA1 establishes DNA damage signaling and pericentric heterochromatin of the X chromosome in male meiosis. *J Cell Biol* 205:663–675.